SCIENTIFIC JOURNAL
EARTH'S CRYOSPHERE

Earth`s Cryosphere, 2015, vol. XIX, No. 1, pp. 11–19 **http://earthcryosphere.ru/**

PERMAFROST MONITORING AND PREDICTIONS

HYDROLOGICAL MODELING: HEAT DYNAMICS IN A SOIL PROFILE (*Part 1*)

Yu.B. Vinogradov, O.M. Semenova[1,2,3], T.A. Vinogradova[3]

[1]*State Hydrological Institute, 23, 2nd Line, V.O., St. Petersburg, 199053, Russia*
[2]*Gidrotekhproekt Ltd, 44-2, pr. Toreza, St. Petersburg, 194223, Russia*
[3]*St. Petersburg State University, 33-35, 10th Line, V.O., St. Petersburg, 199178, Russia; omakarieva@gmail.com*

A new simulation method for soil heat dynamics, integrated into the *Hydrograph* deterministic hydrological model, is based on several simplifying techniques. Namely, it reduces the system of differential equations for thermal conductivity in a soil profile to linear algebraic equations, without sacrifice to quality. Special approaches are used to estimate thermal conductivity and heat transfer in freezing and thawing soils of variable water contents. The model parameters include physical properties of soil layers, such as density, porosity, thermal conductivity, specific heat, and maximum water-holding capacity. The measured properties of soils in different landscapes can be generalized and systematized and further used for reference in hydrological modeling of similar ungauged watersheds without calibration. The new method is verified against a time series of soil temperatures at depths of 20, 40, 80 and 160 cm measured at a site within the Kolyma Water Balance Station.

Thermal conductivity equation, permafrost, hydrological modeling, soil profile, temperature, Kolyma water balance station

INTRODUCTION

Development of permafrost areas in Siberia and extreme North requires solving practical engineering problems of hydrological runoff assessment in poorly gauged watersheds, as well as prediction of future changes to water budget under natural and man-caused climate variations.

Runoff simulations for such areas have to account for both surface and subsurface heat budget in soil profiles exposed to seasonal freezing and thawing because active layer dynamics influences strongly the hydrological responses of permafrost [*Kuchment et al., 2000; Zhang et al., 2000; Gusev and Nasonova, 2010*]. Continuous calculations of depth-dependent soil conditions with variable temperature and water (ice) contents, at a certain time step, are applied to describe water infiltration into frozen soil, surface-subsurface flow interactions, and seasonal runoff redistribution due to freezing of rain or to meltwater infiltration in soil.

Models of soil heat dynamics should allow for specificity of active layer conditions in different landscapes and, on the other hand, should trade off between avoiding calibration of model parameters [*Pomeroy et al., 2007; Semenova, 2010; Vinogradov and Vinogradova, 2010; Vinogradov et al., 2011*] and coping with limited datasets from hardly accessible high-latitude territories in Russia and worldwide [*Semenova and Vinogradova, 2009*].

There are several approaches to soil heat transfer modeling for hydrological applications. This consideration does not include simplified models with freezing and thawing described implicitly, e.g., with empirical relationships between thaw depth and air temperatures [*Nelson et al., 1997*] or with different controls of soil infiltration properties [*Pomeroy et al., 2007*].

Heat dynamics in soils is most often simulated using finite-difference or finite-element solutions to the thermal conductivity equation [*Kuchment et al., 2000*]:

$$\frac{\partial\theta}{\partial t}=\frac{\lambda}{\rho c}\frac{\partial^2\theta}{\partial x^2}, \qquad (1)$$

where θ is the ground temperature, °C; t is the time, s; x is the vertical coordinate, m; λ is the thermal conductivity, W/(m·°C); ρ is the density, kg/m^3; c is the specific heat, J/(kg·°C).

Equation (1) is restricted to soil thermal conductivity and accounts neither for heat consumed by phase change nor for heat input from outside (e.g., with infiltrating water). An efficient numerical technique providing accurate solutions for moving interfaces with regard to phase change was suggested by *Goodrich* [*1978*] and became broadly used later [*Arzhanov et al., 2007*].

Such simulations obviously require costly computations, and special procedures are tried to make

them easier and more stable [*Bowling et al., 2008*], or simpler solutions are sought to the thermal conductivity equation for freezing-thawing soil [*Gusev and Nasonova, 2010*].

The new way of modeling heat dynamics presented below is based on several simplifying techniques that reduce the system of differential equations to linear algebraic equations, without sacrifice to quality. Thermal conductivity and heat transfer are computed within model soil and snow layers showing variable temperature and water content patterns, using algorithms designed for hydrological modeling and integrated into the *Hydrograph* deterministic model [*Vinogradov, 1988; Vinogradov and Vinogradova, 2010*]. The model parameters include different physical properties of soil layers. The new method is verified against a time series of soil temperatures at depths of 20, 40, 80 and 160 cm measured at a site within the Kolyma Water Balance Station.

HEAT DYNAMICS IN A SOIL PROFILE

In the general case, a soil profile consists of frozen and unfrozen layers with seasonally moving, appearing, and disappearing interfaces, which increases the number of equations in system (1) and poses problems to computation. We suggest a new approach to cope with the problem, and to reduce the computation costs for multiple solutions at many points within a watershed and at many time steps.

In classical numerical methods, thermal conductivity equations are solved by computing a continuous temperature profile of points spaced at the step ∂x. In the new method, the step becomes an averaging interval, and a histogram of depth-dependent soil temperatures is used instead of a continuous curve, while the estimated temperatures are assigned to the middle of soil or snow layers.

With the assumption that heat flows $q_{i-1,\,i}$ between simulation layers are proportional to their temperature difference at the coefficients corresponding to heat transfer between soil (snow) and air (ψ) and between neighbor soil layers (ξ, W/(m^2·°C)), the system of classical differential equations for a soil profile of n layers is

$$\begin{aligned} dU_1/dt &= \psi(\eta-\theta_1)-\xi_{12}(\theta_1-\theta_2),\\ dU_i/dt &= \xi_{i-1,i}(\theta_{i-1}-\theta_i)-\xi_{i,i+1}(\theta_i-\theta_{i+1}),\\ dU_n/dt &= \xi_{n-1,n}(\theta_{n-1}-\theta_n)-\xi_{gr}(\theta_n-\theta_{gr}), \end{aligned} \qquad (2)$$

where U_i is the heat stored in the i-th model layer, J; η and θ_i are the air and soil layer temperatures, respectively, °C; $\xi_{i-1,\,i}$ and ξ_{gr} are the coefficients of heat transfer between neighbor soil layers and across the soil profile base, W/(m^2·°C); ψ is the coefficient of heat transfer between air and soil (snow) surface, W/(m^2·°C). The ground temperature at the soil profile base (θ_{gr}, °C) is

$$\theta_{gr} = k_1\theta_c + (1-k_1)\theta_n,$$

where θ_c is the temperature at the constant depth $x_c > x_n$ (x_n is the depth of the lower soil layer). Depending on the depth x_c, the temperature θ_c may be either constant or approximated by

$$\theta_c = \bar{\theta}_c + M\sin(2\pi t/T + Am), \qquad (3)$$

where M is the θ_c amplitude; T is the period (365 day); Am is the initial phase at $t_0 = 0$. The parameter k_1 is estimated by linear interpolation

$$k_1 = 0.5\Delta x_n \big/ (x_c - x_{gr}) \qquad (4)$$

or by minimizing misfit between computed and measured temperatures at the depth x_n. The variables in (4) are: Δx_n is the thickness of the lower soil layer, m; x_c is the depth of soil temperature variations assumed to be the climate norm, m; x_{gr} is the depth of the soil profile base, m.

The soil (snow) – air heat transfer accounts for convection at the solid-air interface, as well as for some other effects.

Solving the system of differential equations for few layers (e.g., $n = 10$) is easy. Integration of (2) being possible only numerically, we suggest several techniques of reducing the differential equation system to the linear algebraic one.

In almost all hydrological models, the air temperature η is used as an input value and is assumed constant within a time step. Let this be valid for both air and soil. Assume that that the top and bottom of each soil layer contact a medium having conventionally constant temperature during the time step Δt.

This leads to the system of differential equations

$$\begin{aligned} dU_1/dt &= \psi(\bar{\eta}-\theta_1)-\xi_{12}(\theta_1-\bar{\theta}_2),\\ dU_i/dt &= \xi_{i-1,i}(\bar{\theta}_{i-1}-\theta_i)-\xi_{i,i+1}(\theta_i-\bar{\theta}_{i+1}),\\ dU_n/dt &= \xi_{n-1,n}(\bar{\theta}_{n-1}-\theta_n)-k_1\xi_{gr}(\theta_n-\bar{\theta}_{gr}), \end{aligned}$$

which can be written as

$$\begin{aligned} dU_1/dt &= \psi\bar{\eta}-(\psi+\xi_{12})\theta_1+\xi_{12}\bar{\theta}_2,\\ dU_i/dt &= \xi_{i-1,i}\bar{\theta}_{i-1}-(\xi_{i-1,i}+\xi_{i,i+1})\theta_i+\xi_{i,i+1}\bar{\theta}_{i+1}, \qquad (5)\\ dU_n/dt &= \xi_{n-1,n}\bar{\theta}_{n-1}-(\xi_{n-1,n}+k_1\xi_{gr})\theta_n+k_1\xi_{gr}\bar{\theta}_{gr}. \end{aligned}$$

The heat (U_i, J) stored in the i-th layer is

$$U_i = c\rho\Delta x\theta, \qquad (6)$$

where x is the vertical coordinate, m; ρ is the density, kg/m^3; c is the specific heat, J/(kg·°C) of the given layer. According to (6), the heat U_i, can be used instead of the soil layer temperature in (5):

$$\frac{dU_1}{dt}=\psi\bar{\eta}-\frac{\psi+\xi_{12}}{c_1\rho_1\Delta x_1}U_1+\frac{\xi_{12}}{c_2\rho_2\Delta x_2}\bar{U}_2,$$
$$\frac{dU_i}{dt}=\frac{\xi_{i-1,i}}{c_{i-1}\rho_{i-1}\Delta x_{i-1}}\bar{U}_{i-1}-$$
$$-\frac{\xi_{i-1,i}+\xi_{i,i+1}}{c_i\rho_i\Delta x_i}U_i+\frac{\xi_{i,i+1}}{c_{i+1}\rho_{i+1}\Delta x_{i+1}}\bar{U}_{i+1}, \quad (7)$$
$$\frac{dU_n}{dt}=\frac{\xi_{n-1,n}}{c_{n-1}\rho_{n-1}\Delta x_{n-1}}\bar{U}_{n-1}-\frac{\xi_{n-1,n}+k_1\xi_{gr}}{c_n\rho_n\Delta x_n}U_n+k_1\xi_{gr}\theta_{gr}.$$

With the notations

$$A_1=\psi\bar{\eta},\ B_1=\frac{\psi+\xi_{12}}{c_1\rho_1\Delta x_1},\ D_1=\frac{\xi_{12}}{c_2\rho_2\Delta x_2}\bar{U}_2,$$
$$A_i=\frac{\xi_{i-1,i}}{c_{i-1}\rho_{i-1}\Delta x_{i-1}}\bar{U}_{i-1},\ B_i=\frac{\xi_{i-1,i}+\xi_{i,i+1}}{c_i\rho_i\Delta x_i},$$
$$C_i=\frac{\xi_{i,i+1}}{c_{i+1}\rho_{i+1}\Delta x_{i+1}}\bar{U}_{i+1}, \quad (8)$$
$$A_n=\frac{\xi_{n-1,n}}{c_{n-1}\rho_{n-1}\Delta x_{n-1}}\bar{U}_{n-1},\ B_n=\frac{\xi_{n-1,n}+k_1\xi_{gr}}{c_n\rho_n\Delta x_n},\ D_n=k_1\xi_{gr}\theta_{gr},$$

system (7) for any soil layer can become

$$dU/(A-BU+D)=dt,$$
$$\int_{U_0}^{U^*}\left[\frac{dU}{A-BU+D}\right]=\int_{t_0}^{t}dt, \quad (9)$$
$$U^*=\left[1-\exp(-B\Delta t)\right]\frac{A+D}{B}+U_0\exp(-B\Delta t),$$

where U_0 and U^* refer to the heat (J) stored in the soil layer at the times t_0 and t, respectively; Δt is the time step, s.

System (9) appears to be workable only in the absence of phase change, but individual soil layers subject to freezing and thawing consume or release heat and thus maintain constant $U^* = 0$, while the number of such layers may vary.

Equations (9) written in a more convenient form become

$$\Delta U=\left[1-\exp(-B\Delta t)\right]\left[(A+D)/B-U_0\right], \quad (10)$$

where $\Delta t = U^* - U_0$ defines the heat loss for temperature or phase changes or sums up the two processes. This approach provides an invariable number of equations in the system where only coefficients change in the case of phase changes. Let $\bar{U}$ in systems (7) and (8) be an effective average value intermediate between U^* and U_0, given by

$$\bar{U}=U_0+k_2\Delta U,$$

where $0 < k_2 < 1$. The weight coefficient k_2 is estimated as a function of the time step Δt using the relationship obtained by *Litvin* [*1991*] from numerical results for different time steps in simple test solutions:

$$k_2 = 1 - 0.5 \exp(-10^{-5}\Delta t).$$

For $\Delta t = 1$ day, $k_2 = 0.79$.

The coefficients in (8), according to (10), are brought together into a system of parametric groups

$$R_1=1-\exp\left[-(\psi+\xi_{12})\Delta t/(c_1\rho_1\Delta x_1)\right],$$
$$N_1=R_1\bar{\eta}\psi c_1\rho_1\Delta x_1/(\psi+\xi_{12}),$$
$$M_1=k_2R_1\xi_{12}c_1\rho_1\Delta x_1/\left[(\psi+\xi_{12})c_2\rho_2\Delta x_2\right],$$
$$L_1=M_1(U_2)_0/k_2-R_1(U_1)_0,$$
$$R_i=1-\exp\left[-(\xi_{i-1,i}+\xi_{i,i+1})\Delta t/(c_i\rho_i\Delta x_i)\right],$$
$$N_i=k_2R_i\xi_{i-1,i}c_i\rho_i\Delta x_i/\left[(\xi_{i-1,i}+\xi_{i,i+1})c_{i-1}\rho_{i-1}\Delta x_{i-1}\right],$$
$$M_i=k_2R_i\xi_{i,i+1}c_i\rho_i\Delta x_i/\left[(\xi_{i-1,i}+\xi_{i,i+1})c_{i+1}\rho_{i+1}\Delta x_{i+1}\right], \quad (11)$$
$$L_i=\left[N_i(U_{i-1})_0+M_i(U_{i+1})_0\right]/k_2-R_i(U_i)_0,$$
$$R_n=1-\exp\left[-(\xi_{n-1,n}+k_1\xi_{gr})\Delta t/(c_n\rho_n\Delta x_n)\right],$$
$$N_n=k_2R_n\xi_{n-1,n}c_n\rho_n\Delta x_n/\left[(\xi_{n-1,n}+k_1\xi_{gr})c_{n-1}\rho_{n-1}\Delta x_{n-1}\right],$$
$$M_n=R_n\theta_ck_1\xi_{gr}c_n\rho_n\Delta x_n/(\xi_{n-1,n}+k_1\xi_{gr}),$$
$$L_n=N_n(U_{n-1})_0/k_2-R_n(U_n)_0,$$

which are coefficients of the system of linear algebraic equations

$$\Delta U_1 = N_1 + M_1\Delta U_1 + L_1,$$
$$\Delta U_i = N_i + M_i\Delta U_{i-1} + M_i\Delta U_{i+1} + L_i, \quad (12)$$
$$\Delta U_n = N_n\Delta U_{n-1} + M_n + L_n.$$

The tridiagonal band matrix of the system makes the calculations easier.

If phase change occurs in the given or neighbor soil layers, the heat they store is zero, this leading to some simplification. At phase change in the upper $(i - 1)$-th soil layer (for the uppermost layer it corresponds to $\bar{\eta}=0$), systems (11) and (12) reduce to

$$\Delta U_i=M_i\Delta U_{i+1}+L_i,$$
$$L_i=M_i(U_{i+1})_0/k_2-R_i(U_i)_0; \quad (13)$$

if phase change occurs in the lower $(i + 1)$-th layer, they become

$$\Delta U_i=N_i\Delta U_{i-1}+L_i,$$
$$L_i=N_i(U_{i-1})_0/k_2-R_i(U_i)_0. \quad (14)$$

or, at phase changes taking place simultaneously in both layers,

$$\Delta U_i = L_i, \quad L_i = -R_i(U_i)_0. \tag{15}$$

The phase change restricted to the i-th layer is described by the coefficients

$$N_1 = \bar{\eta}\psi\Delta t,\ M_1 = k_2\xi_{12}\Delta t/(c_2\rho_2\Delta x_2),\ L_1 = M_1(U_2)_0/k_2,$$
$$N_i = k_2\xi_{i-1,i}\Delta t/(c_{i-1}\rho_{i-1}\Delta x_{i-1}),$$
$$M_i = k_2\xi_{i,i+1}\Delta t/(c_{i+1}\rho_{i+1}\Delta x_{i+1}), \tag{16}$$
$$L_i = \left[N_i(U_{i-1})_0 + M_i(U_{i+1})_0\right]/k_2,$$
$$N_n = k_2\xi_{n-1,n}\Delta t/(c_{n-1}\rho_{n-1}\Delta x_{n-1}),\ M_n = k_1\xi_{gr}\theta_c\Delta t,$$
$$L_n = N_n(U_{n-1})_0/k_2.$$

If both the given and neighbor soil layers undergo phase changes simultaneously, heat transfer between them is zero:

$$N_i = M_i = L_i = 0. \tag{17}$$

The time step Δt can be split when both temperature and phase changes occur within it in a single soil layer. In this case, the dominant process is chosen for a small part of Δt while the inferior process is neglected. In profiles with a snow layer, the latter substitutes for the upper soil layer and is assumed to have a variable thickness (Δx_c, m) and the respective thermal properties and water content.

THERMAL CONDUCTIVITY AND HEAT TRANSFER IN SOIL AND SNOW LAYERS

In thermal conductivity simulations, a multiphase dispersive soil is assumed to consist of a solid and a gas (air) phases. Air is an absolute thermal insulator, which reduces the cross section of a conventional unit soil column; furthermore, it deforms or breaks down the heat conducting paths in the system, which additionally decreases the thermal conductivity of the whole column. Let the effective thermal conductivity of such a system (dry soil) be proportional to the power function of the solid fraction:

$$\lambda_m = \lambda_0(1-\varepsilon)^m,\ m>1, \tag{18}$$

where λ_0 is the thermal conductivity, W/(m·°C); ε is the soil porosity, m^3/m^3; m is the constant.

Table 1. **Specific heat c and thermal conductivity λ_0 of different soil types**

Soil	c, J/(kg·°C)	λ_0, W/(m·°C)
Sand	780	2.5
Silt	830	1.7
Clay silt	840	1.3
Clay	880	1.0
Peat	1930	0.8

If water substitutes for all air in soil, heat transfer will involve many heat conducting elements of two types connected in series, in parallel, or in different combinations of the two. In the case of serially connected elements (the left superscript is –1), layer heat flows equalize, and the equation for the total thermal conductivity λ_M of soil with water-filled porosity is

$$^{-1}(\lambda_M) = \lambda_0\lambda^\bullet/\left[\lambda_0\varepsilon + \lambda^\bullet(1-\varepsilon)\right] = \left[(1-\varepsilon)/\lambda_0 + \varepsilon/\lambda^\bullet\right]^{-1}, \tag{19}$$

where $\lambda^\bullet$ is the thermal conductivity of water, W/(m·°C). In the case of parallel element connection (the left superscript is 1),

$$^{1}(\lambda_M) = \lambda_0(1-\varepsilon) + \lambda^\bullet\varepsilon. \tag{20}$$

In fact, various connections make up an intermediate complex combination. Equations (19) and (20) are for calculating harmonic and arithmetic weighted means at $^{-1}(\lambda_M) \le {}^{1}(\lambda_M)$, but there is the geometric mean $^{-1}(\lambda_M) \le \lambda_M \le {}^{1}(\lambda_M)$, between the harmonic and arithmetic means, and the equation for λ_M becomes

$$(\lambda_M) = \lambda_0^{1-\varepsilon} + \left(\lambda^\bullet\right)^{\varepsilon}. \tag{21}$$

Equations (18) and (21) give simple interpolation estimates of thermal conductivity for a multiphase medium:

$$\lambda = (\lambda_M - \lambda_m)(\omega)^n + \lambda_m,\ n<1, \tag{22}$$

where $\omega = u/\varepsilon$ is the relative water (ice) content, m^3/m^3; u is the bulk water (ice) content of the soil layer, m^3/m^3.

The soil layer subject to phase change consists of at least two sublayers, each with its thermal conductivity, though effective properties were assigned to it over the whole Δx. Therefore, the thermal conductivity of this layer λ_i is found as a harmonic mean, with the relative weight coefficients of water and ice fractions:

$$\lambda_i = u_i^\bullet/\left[\lambda_i^\bullet\left(u_i^\bullet + u_i^*\right)\right] + u_i^*/\left[\lambda_i^*\left(u_i^\bullet + u_i^*\right)\right],$$
$$\lambda_i^\bullet = \left(\lambda_M^\bullet - \lambda_m\right)\left[\left(u_i^\bullet + u_i^*\right)/\varepsilon_i\right]^n + \lambda_m, \tag{23}$$
$$\lambda_i^* = \left(\lambda_M^* - \lambda_m\right)\left[\left(u_i^\bullet + u_i^*\right)/\varepsilon_i\right]^n + \lambda_m,$$

where $u_i^\bullet$, u_i^* are the bulk water and ice contents of the soil layer, respectively, m^3/m^3; $\lambda_i^\bullet$, λ_i^* are the thermal conductivities of the wet ice-rich soil layer, W/(m·°C); $\lambda_M^\bullet$, λ_M^* are the thermal conductivities of the soil layer with 100 % water- or ice-filled porosity, W/(m·°C); n is the constant.

We recommend the constants m = 2.5 in (18) and n = 0.75 in (23). The standard values λ_0 used in (18) are listed in Table 1.

Heat transfer coefficients vary in time and space as a function of several factors, but are assumed to be invariable within Δt and are calculated according to the initial soil state. Heat transfer and thermal conductivity are calculated using successively written equations for steady-state heat flow (q, W/m^2) between air and ground surface, between ground surface and a point at the depth ($\Delta x_1/2$, m) below this surface, and between air and this point:

$$q=\alpha(\theta_0-\eta),\ q=2\lambda(\theta-\theta_0)/\Delta x,\ q=\psi(\theta-\eta), \quad (24)$$

where θ_0 is the surface temperature, °C. Then,

$$\psi=1/[\Delta x/2\lambda+1/\alpha]. \quad (25)$$

The parameter α, W/(m^2·°C), refers to heat input to the surface and can be interpreted as heat transfer between air and upper soil layer at $\lambda\to\infty$, i.e., provided that heat flows are away from the interface immediately. The value ψ never exceeds $2\lambda/\Delta x$ at any α, i.e., the heat transfer ψ is limited from above only by the possibility of depthward heat flow into the soil. The α values range from 1.0 to 5.0 W/(m^2·°C) depending on climate and vegetation type: 1–2 for severe cold climate; $1\to1.5\to2$ for forest–tundra–vegetation-free surface; 3–4 for moderate climate; $3\to4$ for forest and open landscapes; 5 for warm climate. The parameter α requires calibration by fitting the predicted temperatures to the observed values, but it is stable across landscapes. For northeastern Russia, its recommended values are 1 or 2 depending on landscape.

In the same way as in (25), heat transfer between two soil layers is

$$\xi_{i,i+1}=2/(\Delta x_i/\lambda_i+\Delta x_{i+1}/\lambda_{i+1}),$$

and that between air and snow is

$$\psi_c=1/[\Delta x_c/2\lambda_c+1/\alpha_c], \quad (26)$$

where Δx_i, Δx_c are the thicknesses of soil and snow layers, respectively, m; λ_i, λ_c are the thermal conductivities of soil and snow layers, respectively, W/(m^2·°C). The heat flow to the snow surface at negative air temperatures (α_c) is assumed to be 5.0 W/(m^2·°C).

The thermal conductivity of dry snow can be found using (18), with ice as the solid:

$$\lambda_c^*=\lambda^*(1-\varepsilon_c)^m=\lambda^*\left(\gamma_c^*/\rho^*\right)^m, \quad (27)$$

where λ^*, λ_c^* are the thermal conductivities of ice and dry snow, respectively, W/(m·°C); ε_c is the porosity of snow, m^3/m^3; ρ^* and γ_c^* are the densities of ice and snow, kg/m^3; m is the constant.

The effective thermal conductivity depends on snow temperature. Given that the effect of convection is inversely proportional to snow density, the calculation is done using the equation [*Vinogradov, 1988*]

$$\lambda_c^*\left(\theta_c,\gamma_c^*\right)/\lambda_c^*=1+\exp(k_3\theta_c)\left(1-\gamma_c^*/\rho^*\right), \quad (28)$$

where $\theta_c<0$ °C is the snow temperature, °C; $k_3=0.1$ is the constant. Thus, at negative snow temperatures, the thermal conductivity of dry snow (λ_c^*) is found using (27) with the factor (28) and the small additional term

$$\lambda_c^*=\left[1+\exp(k_3\theta_c)\left(1-\gamma_c^*/\rho^*\right)\right]\left[\lambda^*\left(\gamma_c^*/\rho^*\right)^m+0.02\right].$$

The thermal conductivity of wet snow is found using an equation similar to (22):

$$\lambda_c=\left[(\lambda_c)_M-\lambda_c^*\right]\omega_c^n+\lambda_c^*,$$

$$(\lambda_c)_M=\lambda^*(1-\varepsilon_c)+\lambda^{\bullet}\varepsilon_c=\left(\lambda^*-\lambda^{\bullet}\right)\gamma_c^*/\rho_c+\lambda^{\bullet},$$

where $(\lambda_c)_M$ is the thermal conductivity of snow with 100 % water-filled porosity (a fictitious value), W/(m·°C); $\omega_c=u_c/\varepsilon_c$ is the water-filled porosity of snow, m^3/m^3; u_c is the bulk water content of snow, m^3/m^3; n is the constant. The fictitious thermal conductivity of wet snow $(\lambda_c)_M$ is used only to calculate heat transfer between snow und the uppermost soil layer with (24) and between air and freezing snow according to (26). The snow water content is assumed to be homogeneous and isotropic.

In the case of positive air temperatures and snow melting (when all heat received by snow is spent on phase change), the heat transfer is assumed to be equal to heat input (α_c^+), and is related to snow melting as

$$\psi_c^+=\alpha_c^+=l^*\rho^{\bullet}\zeta,$$

where l^* is the specific heat of ice melting, J/kg, and ζ is the snow melting coefficient, m/(°C·s).

SIMULATION WORKFLOW

In the presence of snow, the model specifies initial conditions, namely, the initial total moisture it stores, density, temperature, and water content in snow exposed to melting (0 °C); initial mean temperature and water (ice) content are required for each soil layer. If no exact constraints on the temperature-depth profile are available, uniform temperature is assumed with regard to freezing or thawing of the active layer by the starting date. The soil temperature equilibrates with the true value soon (within one year of simulation) and then causes no effect on modeling results. The values of mean temperature of air (η) and ground at a certain depth (θ_{gr}) that control heat transfer with the atmosphere and with deeper soil layers are specified for each successive time step, and the respective temperature profiles (θ_i) are calculated for the step end. The resulting values are used for reference as initial conditions for the following time step.

The workflow comprises several units (Fig. 1). Three units calculate the amount of heat (i) stored in

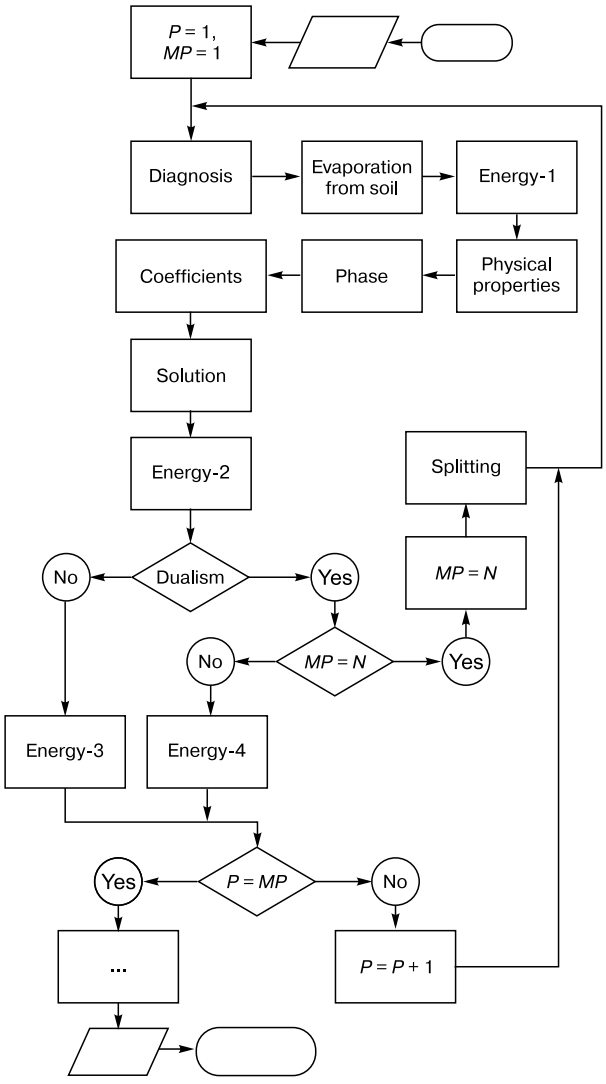

Fig. 1. Simulation workflow.

snow (its presence or absence is detected in the very beginning) after evaporation (*Diagnosis*); (ii) spent for evaporation in each soil layer (*Evaporation from soil*); (iii) required for ice melting or water freezing in each snow and soil layer (*Energy-1*). Six other units are, respectively, for (i) calculating the thermal properties (specific heat, thermal conductivity, and heat transfer) of snow and soil according to equations (18)–(23) with regard to variable water or ice contents (*Physical properties*); (ii) estimating, with (11)–(17), the coefficients *R*, *N* and *L* (*Coefficients*); (iii) calculating heat input to the soil (snow) layer for a time step or its part (*Solution*); (iv) predicting whether the input heat is spent on freezing or thawing in the case of phase change (*Energy-2*); (v) predicting whether the soil (snow) layers undergo one or two (dual) processes (temperature and phase changes) and whether division of the time step is required (*Dualism*); (vi) dividing the time step into the specified number of sub-steps *MP* (*Sub-steps*). As for the latter, the modeling experience shows that *MP* = 10 is enough for most of cases but can be greater if necessary. After dividing the time step, the whole workflow since *Diagnosis* repeats for all sub-steps. If both phase and temperature changes occur within some sub-step, the dominant process is chosen (*Energy-4*), and the inferior process is neglected. *Energy-3* is for estimating the final amount of heat received by a soil (snow) layer without dualism.

RESULTS

The method was verified against a time series of soil temperatures measured at different depths at the meteorologial site Nizhnyaya (Russian for *Lower*) within the Kolyma Water Balance Station in the headwaters of the Kolyma River (Magadan region). The area is located in the zone of continuous permafrost, in severe climate. Ground temperatures at different depths, to 320 cm, were measured at the site for seven years (1974–1980). The site Nizhnyaya lies in a hillocky wetland covered with moss, grass, and shrubs (cowberry and blueberry) [*Observation Reports, 1959–1991*]. The moss-lichen layer, 40–45 cm thick, lies over 15–20 cm of well-drained talus which freezes up at negative temperatures (with low ice contents); the ice-poor talus layer, in turn, overlies an ice-rich one. The top layer accumulates a part of meltwater in spring, which then freezes back repeatedly. The temperature obviously varies with water and ice content throughout the profile. The temperature patterns observed at the site are typical of well-drained soil on southern slopes [*Glotov and Glotova, 2002*].

Table 2. **Properties of different layers in soil profile, Nizhnyaya site, Kolyma Water Balance Station**

Soil type	*h*, cm	ρ, kg/m^3	ε	ω	*c*, J/(kg·°C)	λ, W/(m·°C)
Moss and lichen	0–10	500	0.95	0.35	1700	1.0
Peat	10–20	1950	0.60	0.15	1700	1.0
Transition layer	20–30	2100	0.50	0.11	1200	1.3
Gray clay with shale debris	30–40	2700	0.40	0.10	750	1.7
Shale debris with fine-grained filling	40–200	2700	0.35	0.10	750	1.7

Note. *h* is depth; ρ is density; ε is porosity; ω is maximum moisture storage capacity; *c* is specific heat; λ is thermal conductivity.

The 2 m thick soil profile (at the maximum thaw depth 1.7 m) was simulated as a sequence of 20 layers, 10 cm each. The properties of different layers (Table 2) according to *Observation Reports* [*1959–1991*] and [*Glotov, 2002; Bantsekina, 2003*] were used as parameters in the *Hydrograph* model [*Vinogradov, 1988; Vinogradov and Vinogradova, 2010; Vinogradov et al., 2011*]. For the sake of simplicity, the initial temperature distribution was assumed to be uniform, with a mean of –1 °C for each simulation layer on the starting date of January 1, 1973. Data from the starting year 1973 was not included into analysis. The initial

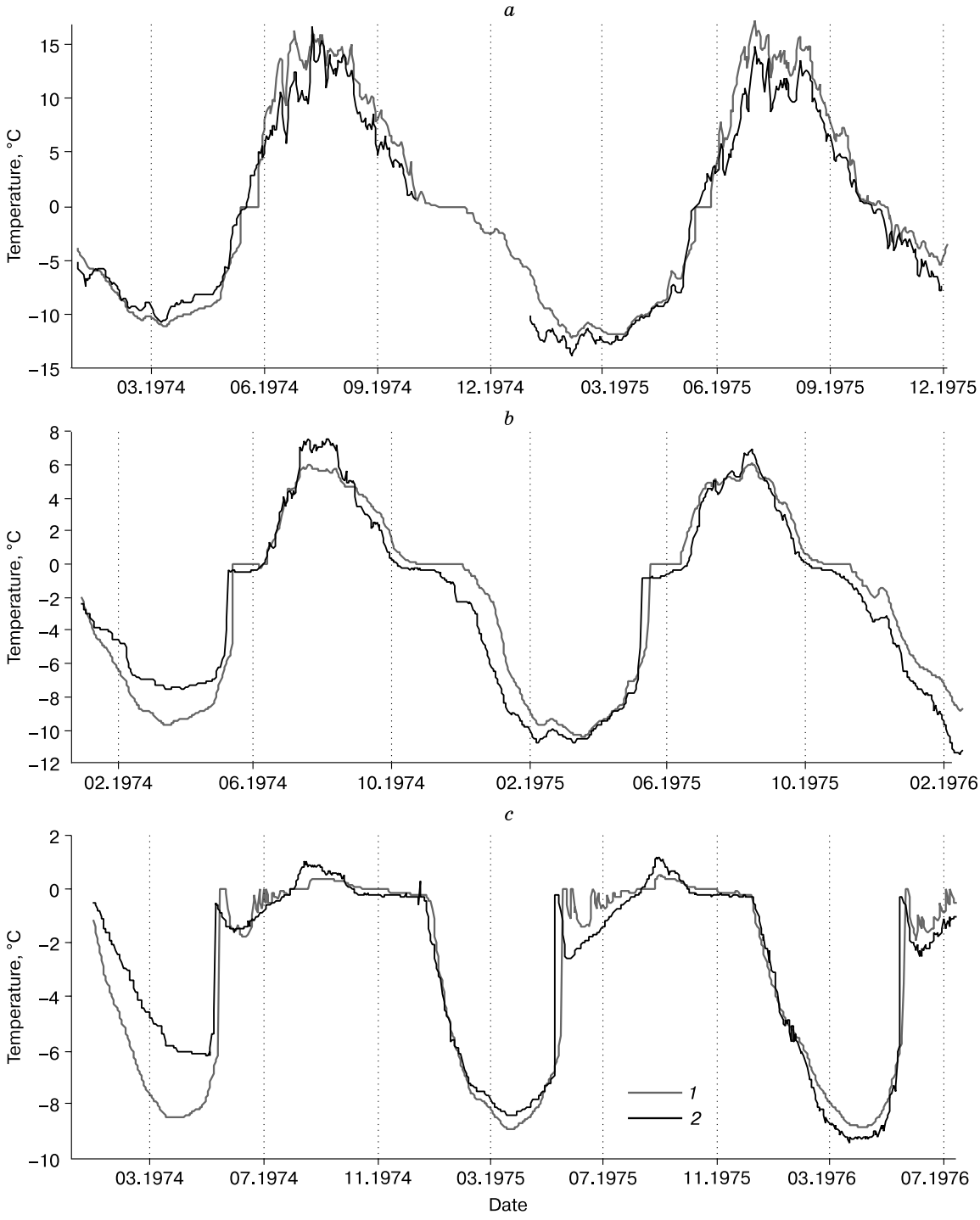

Fig. 2. Simulated (*1*) and observed (*2*) soil temperatures at the depths 20 cm (*a*), 80 cm (*b*), 160 cm (*c*), Kolyma Water Balance Station (1974–1975).

Table 3. **Statistical characteristics of simulated and observed daily ground temperatures (°C) at different depths, Nizhnyaya site**

h, cm	δ, day	T_{obs}, °C	T_{sim}, °C	msd, °C	rms, °C	R^2
20	2099	–2.5	–1.2	1.3	2.4	0.98
40	2070	–3.0	–1.8	1.2	2.4	0.97
80	2736	–3.6	–2.9	0.7	1.6	0.97
160	2859	–3.3	–3.1	0.2	1.3	0.94

Note. h is depth; δ is sample length; T_{obs}, T_{sim} are mean observed and simulated temperatures, respectively; msd is mean systematic deviation; rms is root mean square deviation; R^2 is correlation coefficient.

ice contents of soil layers were specified assuming the ice content equal to the maximum water holding capacity till the summer thaw depth (1.7 m) and to porosity below this depth. Values of model parameters (mean temperature, relative air humidity, and precipitation) measured at the Nizhnyaya site were specified for each time step (24 hr). Annual variations of soil temperature at the depth 3.2 m approximated by equation (3), with $\bar{\theta}_c = -4.0$, $M = 2.8$, $Am = 197$, were used as the lower boundary condition; $k_1 = 0.05$. Snow was considered as a separate layer, and its accumulation and melting was modeled by a special unit in the *Hydrograph* model. Thermal conductivity and specific heat in all soil layers were estimated at each time step, with regard to their water and ice content variations and freezing-thawing cycles.

The simulated and observed mean daily ground temperatures at the depths 20, 80 and 160 cm for 1974–1975 are compared in Fig. 2, *a–c*. The predicted values turn out to exceed the measured temperatures, especially in the summer season. The comparison for the period 1974–1981 (Table 3) shows that the *Hydrograph* model successfully resolves even brief episodes of soil warming as a result of meltwater infiltration into frozen soil in spring.

The reported results demonstrate that the new method is applicable to simulations of heat dynamics in permafrost. Note that the results were obtained with pre-specified parameters, without calibration.

CONCLUSIONS

A new method is suggested to simulate heat dynamics in a soil profile based on simplification to the differential equation of soil thermal conductivity which allows an algebraic solution. The techniques use: (i) constant temperatures averaged over the simulation time step Δt instead of continuous values in neighbor soil layers; (ii) heat excess relative to the beginning of the time step ($\Delta U = U^* - U_0$) as a solution to the system of equations instead of heat in the end of the time step, which allows applying the algorithm to both temperature and phase changes; (iii) effective mean heat intermediate between the initial and final values; (iv) the time step divided into sub-steps in the case of both temperature and phase changes in a layer. The algorithm can estimate thermal conductivity and heat transfer in soil and snow layers subject to freezing and thawing.

The reported algorithm implements the approach first suggested in the 1980–1990s and published earlier [*Vinogradov, 1988; Vinogradov and Vinogradova, 2010*] in terms of the hydrological model *Hydrograph* [*Vinogradov et al., 2011*]. The method was tested and successfully applied to runoff simulations for permafrost landscapes [*Semenova et al., 2013*].

The measured physical properties of soils in the profile are employed as the model parameters in simulations and can be systematized according to landscapes to be further used for reference in hydrological modeling of similar poorly gauged watersheds.

The application of the method to simulation of active layer dynamics will be discussed in more detail in the following publication (Part 2).

The study was supported by grant 12-05-31035_mol_a from the Russian Foundation for Basic Research.

References

Arzhanov, M.M., Eliseev, A.V., Demchenko, P.F., Mokhov, I.I., 2007. Modeling of changes in temperature and hydrological regimes of subsurface permafrost, using the climate data (reanalysis). Kriosfera Zemli XI (4), 65–69.

Bantsekina, T.V., 2003. Spring-Summer Geothermal Regime of the Active Layer in Slope Talus (a Case Study of the Upper Kolyma Plateau). Candidate Thesis, Geography, Yakutsk, 137 pp. (in Russian)

Bowling, L.C., Cherkauer, K.A., Adam, J.C., 2008. Current capabilities in soil thermal representations within a large scale hydrology model. Proc. 9th Intern. Conf. on Permafrost, Fairbanks, Alaska, USA, Inst. Northern Eng., Univ. Alaska, vol. 1, pp. 177–182.

Glotov, V.E., 2002. Groundwater in the Kontaktovy Creek watershed as a runoff control, in: Subarctic Small Mountain Rivers: Runoff Controls (from Data of Kolyma Water Balance Station). SVKNII DVO RAN, Magadan, pp. 105–122. (in Russian)

Glotov, V.E., Glotova, L.P., 2002. Geological, geomorphic, and cryological controls of Kontaktovy Creek surface runoff, ibid, pp. 81–104.

Goodrich, L.E., 1978. Efficient numerical technique for one-dimensional geothermal problem with phase change. Intern. J. Heat Mass Transf. 21, 615–621.

Gusev, E.M., Nasonova, O.N., 2010. Modeling Heat and Water Transport across the Soil-Air Interface. Nauka, Moscow, 327 pp. (in Russian)

Kuchment, L.S., Gelfan, A.N., Demidov, A.I., 2000. Modeling runoff in permafrost watersheds (a case study of the Upper Kolyma). Vod. Resursy 27 (4), 435–444.

Litvin, A.S., 1991. Methods for modeling heat dynamics of a dispersive medium, compared. Transactions GGI, Issue 343, pp. 73–83. (in Russian)

Nelson, F.E., Shiklomanov, N.I., Mueller, G., Hinkel, K.M., Walker, D.A., Bockheim, J.G., 1997. Estimating active layer thickness over a large region: Kuparuk river basin, Alaska, USA. Arctic, Antarctic and Alpine Res. 29 (4), 367–378.

Observation Reports, 1959–1991. Kolyma Water Balance Station, 1948–1990, Issues 1–34. Kolyma UGKS, Magadan. (in Russian)

Pomeroy, J.W., Gray, D.M., Brown, T., Hedstrom, N.R., Quinton, W.L., Granger, R.J., Carey, S.K., 2007. The cold regions hydrological model: a platform for basing process representation and model structure on physical evidence. Hydrol. Process. 21, 2650–2667.

Semenova, O.M., 2010. Experience in modelling runoff formation processes at different scales using data of water-balance stations. IAHS Publ. 336, 167–172.

Semenova, O., Lebedeva, L., Vinogradov, Yu., 2013. Simulation of subsurface heat and water dynamics, and runoff generation in mountainous permafrost conditions, in the Upper Kolyma River basin, Russia. Hydrogeol. J. 21 (1), 107–119, doi:10.1007/s10040-012-0936-1.

Semenova, O.M., Vinogradova, T.A., 2009. An universal approach to runoff processes modelling: coping with hydrological predictions in data-scarce regions. IAHS Publ. 333, 11–19.

Vinogradov, Yu.B., 1988. Runoff Modeling. An Experience of Critical Analysis. Gidrometeoizdat, Leningrad, 312 pp. (in Russian)

Vinogradov, Yu.B., Vinogradova, T.A., 2010. Hydrological Modeling. Akademia, Moscow, 366 pp. (in Russian)

Vinogradov, Yu.B., Semenova, O.M., Vinogradova, T.A., 2011. An approach to the scaling problem in hydrological modelling: the deterministic modelling hydrological system. Hydrol. Process. 25, 1055–1073, doi:10.1002/hyp.7901.

Zhang, Z., Kane, D.L., Hinzman, L.D., 2000. Development and application of a spatially distributed Arctic Hydrologic and Thermal Process Model (ARHYTHM). J. Hydrol. Process. 14 (6), 1017–1044.

Received November 25, 2012